Conformational Study of Some Amino Acid Conjugates of Indol-3-yl-acetic Acid (IAA) by ^{1}H-NOE-Difference Spectroscopy. Structure/Auxin Activity Relationships

Helmut Duddeck, Monika Hiegemann, and Mario F. Simeonov*

Ruhr-Universität Bochum, Fakultät für Chemie, Postfach 102148, D-4630 Bochum 1, Bundesrepublik Deutschland

and

Biserka Kojic-Prodic, Biljana Nigovic, and Volker Magnus

Rudjer-Boskovic Institute, POB 1016, 41001-Zagreb, Yugoslavia

Z. Naturforsch. **44c**, 543–554 (1989); received April 26, 1989

Amino Acid Conjugates

The conformation of the side chain of indol-3-yl-acetic acid conjugates with amino acids (L-alanine, glycine, L-i-leucine, L-α-aminobutyric acid, DL-aspartic acid, DL-phenylalanine, and δ-aminovaleric acid) has been studied by ^{1}H-NMR-NOE-difference spectroscopy. Comparison with the conformation in the solid state is given in the light of structure-activity relationships.

Introduction

Since the structure of the plant growth hormone indol-3-yl-acetic acid (IAA, natural auxin) was established in 1934 [1], considerable efforts have been devoted to the subject of auxin activity [2]. The presence of bound auxin in the seeds of cereals was first demonstrated by Cholodny in 1935 [3]. The derivatives themselves were described by Cohen and Bandurski [4]. To date, bound auxins or auxin conjugates have many times been found in plant material of various origin where they are frequently more abundant than the free hormone [4]. As far as identified, they mostly contain IAA linked by ester, glycosidic, or amide bonds to a host of compounds including even biopolymers. Naturally occurring conjugates of IAA are supposed to be storage forms which are hydrolyzed to the free hormone as required for concerted plant development [4]. Non-natural conjugates have been used as slow-release sources of auxin to manipulate growth and differentiation in plant tissue culture [5]. There are also physiological or pharmacological effects, so far difficult to define, which appear to be caused by the conjugates themselves [6]. More detailed knowledge on their molecular structures, in the solid state and in solution, may provide the clue to their mechanism of action. To produce a biological effect auxin must first be attached to some receptor. There are experiments suggesting that one of the receptor sites is a glycoprotein connected to the plasma membrane [2]; in this sense IAA conjugates are model compounds. At present structural and stereochemical data on IAA, its conjugates and chemically related compounds are scarce. The ^{1}H, ^{13}C NMR and IR data for indolylacetic acids with the side chain attached to position 1, 2, and 3 of the aromatic ring [7], some other 3-substituted indole derivatives [8–10], and N_α-acetyl-N_ε-IAA-L-lysine [11] have been published. NMR spectral assignments for other IAA-amino acid conjugates have not been reported. Moreover, nothing is known about the conformational behaviour of the side chain in these compounds which must play some biological role [2, 12]. Systematic analysis of structural parameters and electronic properties of IAA amino acid conjugates may help to understand their widely different biological activities. The conformational behaviour of the side chain of a number of these compounds in solution (Fig. 1), determined by ^{1}H-NMR-NOE-difference spectroscopy is reported here and compared with the conformation in the solid state.

* Permanent address: Bulgarian Academy of Sciences, Institute of Organic Chemistry, 1113-Sofia, Bulgaria.

Reprint requests to Prof. Dr. H. Duddeck or Dr. B. Kojic-Prodic.

Verlag der Zeitschrift für Naturforschung, D-7400 Tübingen
0341–0382/89/0700–0543 $ 01.30/0

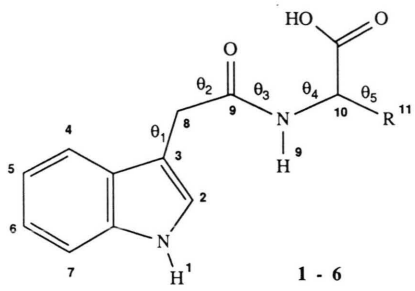

1 - 6

1 : IAA-L-Ala : R = CH_3
2 : IAA-Gly : R = H
3 : IAA-L-Ile : R = $CH(CH_3{}^{14})CH_2{}^{12}CH_3{}^{13}$
4 : IAA-L-Abu : R = $CH_2CH_3{}^{12}$
5 : IAA-DL-Asp : R = CH_2COOH
6 : IAA-DL-Phe : R = CH_2Ph

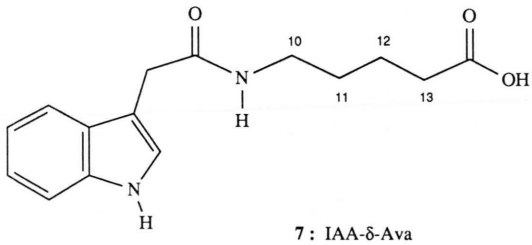

7 : IAA-δ-Ava

Fig. 1. Formulae of amino acid conjugates of indolyl-3-acetic acid (**1**–**7**).

Experimental

A general method to prepare amino acid conjugates of IAA is the aminolysis of the mixed anhydride formed from indol-3-yl-acetic acid and ethyl chloroformate [13]. According to the extension and modification [5] of this method most of the common L-amino acid conjugates have been synthesized [6]. Syntheses of IAA-DL-Asp (**5**) and IAA-δ-Ava (**7**) were performed according to those in references 14 and 15, respectively.

NMR spectra were obtained at ambient temperature on a Bruker AM-400 spectrometer operating at 400.1 MHz (^{1}H) equipped with an Aspect 3000 computer. Sample concentrations were about 0.1 to 0.3 M in dimethylsulphoxide-d_6. All chemical shifts were referenced to the solvent (δ = 2.49). Samples were not degassed.

The steady-state NOE-difference spectra were measured using a standard pulse sequence in which the subtraction is done by 0°/180° phase shifts. We used the minimal decoupler power required to observe a maximal magnitude of NOE enhancements with an irradiation time of two times the proton relaxation time $T_1(^1H)$ and a delay five times the $T_1(^1H)$ of the proton of interest. At these conditions minimal artifacts (SPT-effects) were also observed. Typical parameters were a 4500 Hz spectral width, 32 scans for each position of irradiation and 16 K data points. The NOE magnitude is the ratio (in per cent) of the positive integral intensity relative to the negative one at the irradiation position observed in NOE-difference spectrum. The signal-to-noise ratio was sufficient to obtain NOEs within an experimental error of ± 1%.

Preliminary $T_1(^1H)$ values were determined using the standard inversion recovery pulse sequence with a 10 s delay between the transients. The pulse intervals varied incrementally from 0.1 s to 15 s. The 90° pulse width was 12.5 μs. The data acquired were analyzed by the computer.

Results and Discussion

Conformation of the side chain in the solid state (X-ray data)

The X-ray structure analysis of IAA-L-Ala (**1**, Fig. 2), IAA-L-Ile (**3**, Fig. 3), IAA-DL-Asp (**5**, Fig. 4) and IAA-δ-Ava (**7**, Fig. 5) has revealed the conformation of the side chain [16]. Torsion angles, defining its conformation, determined from X-ray and NMR data are given in Table I.

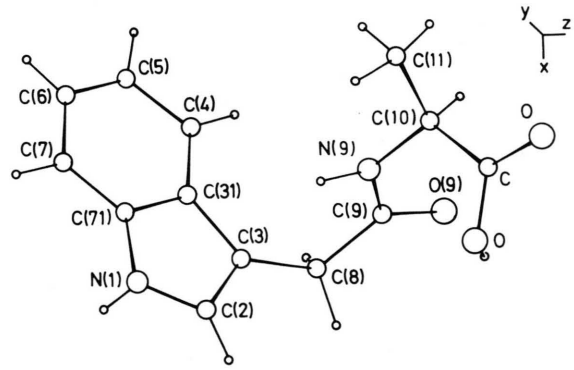

Fig. 2. Perspective view of **1** illustrating the conformation in the solid state.

Table I. Torsion angles (deg) in some IAA-amino acid conjugates; X-ray (1. entry) and NMR* data from this work (2. entry).

	1	**3**	**5**
θ_1 C2–C3–C8–CO	−111.2/−80 ± 10	110.3/∓90	−113.0/−90
θ_2 C3–C8–CO–NH	6.9/0 & 180	− 18.7/∓0 & 180	20.9/0 & 180
θ_3 C8–CO–NH–C10	174.6/180	177.2/−	−174.0/−
θ_4 CO–NH–C10–COOH	− 76.3/−80	− 78.4/−80	−158.5/−160
H9–NH–C10–H10	−155/0–40	151/≈150	180/−

* Signs are derived from the molecular model.

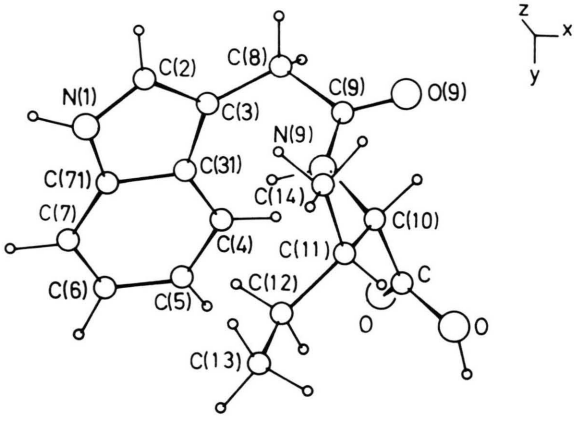

Fig. 3. Perspective view of **3** illustrating the conformation in the solid state.

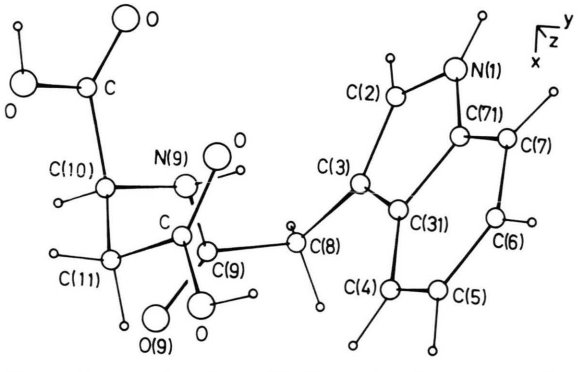

Fig. 4. Perspective view of **5** illustrating the conformation in the solid state.

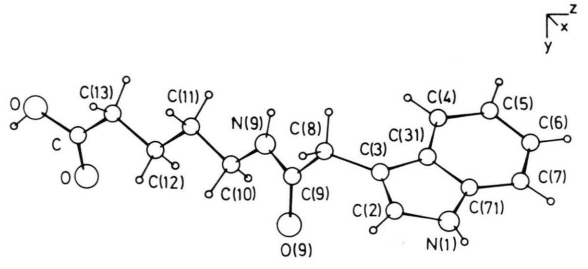

Fig. 5. Perspective view of **7** illustrating the conformation in the solid state.

In these structures the side chain is close to be perpendicular to the indole ring plane (θ_1 in Table I) with some slight tilt towards the benzene ring (for **1**, **3**, and **5**). The NH-amide group faces the indole ring (above C3 atom, $-18.7° < \theta_2 < 20.9°$), while the carbonyl group is in the opposite direction (C3–C8–C9–O torsion angle being −179.7° for **1**, −162.9° for **3** and −160.2° for **5**). However, in the crystal structure of **7**, the conformation about θ_2 (−135.3(5)°) is different. The orientation around θ_3 is *trans (E)* (Table I, Fig. 2 and 6–9). The intramolecular hydrogen bonds in the crystal structures of IAA-L-Ala (**1**) and IAA-DL-Asp (**5**) reduce the flexibility along the NH–C10 bond: in the crystal structure of **1** the O=C–OH ··· O=C type and in **5** the NH ··· O=C–OH type involving the peptide nitrogen [16].

^{1}H NMR measurements

The ^{1}H NMR spectral assignment was performed on the basis of chemical shifts, signal intensities, multiplicities and NOEs. The results are given in the Tables II–VIII.

Table II. ^{1}H NMR data (δ, *J*, T_1 and NOE) of IAA-L-Ala (**1**), in DMSO-d_6.

Proton	Chemical shift δ [ppm]	Coupling constant *J* [Hz]	Relax. time T_1 [s]	Nuclear Overhauser effects* NOE [%]
H1	10.82	–	1.0	10 (H2), 5 (H7)
H2	7.18	2.3 (H1)	2.1	2 (H8, 8′), 8 (H1)
H4	7.55	7.8 (H5)	1.5	17 (H5)
H5	6.96	7.8 (H4), 1.1 (H7), 9.8 (H6)	1.5	8 (H6), 10 (H4)
H6	7.05	8.1 (H7), 1.2 (H4), 9.8 (H5)	1.6	2 (H5), 8 (H7)
H7	7.32	8.1 (H6)	2.4	10 (H6), 4 (H1)
H8, 8′	3.52	1.8 (H2)	0.5	5 (H2), 6 (H4), 8 (H9)
H9	8.23	7.3 (H10)	0.6	5 (H11), 7 (H8, 8′), 5 (H10), 2 (H4), 2 (H2)
H10	4.20	7.3 (H11, H9)	1.8	3 (H9), 8 (H11)
H11	1.26	7.3 (H10)	0.5	5 (H9), 12 (H10)

* NOEs observed for the signals indicated when the proton at the left-hand side of the row is irradiated.

Table III. ^{1}H NMR data (δ, *J*, T_1 and NOE) of IAA-Gly (**2**), in DMSO-d_6.

Proton	Chemical shift δ [ppm]	Coupling constant *J* [Hz]	Relax. time T_1 [s]	Nuclear Overhauser effects* NOE [%]
H1	10.86	–	0.9	12 (H2), 7 (H7)
H2	7.20	2.3 (H1)	2.1	10 (H1), 2 (H8, 8′), 1 (H9)
H4	7.54	7.9 (H5)	1.9	3 (H8, 8′), 15 (H5)
H5	6.94	1.1 (H7), 8.1 (H4, H6)	1.5	14 (H4), 12 (H6)
H6	7.04	0.7 (H4), 7.9 (H5, H7)	1.4	7 (H5), 11 (H7)
H7	7.33	8.1 (H6)	2.2	5 (H1), 10 (H6)
H8, 8′	3.56	–	0.5	8 (H2), 7 (H4), 7 (H9)
H9	8.16	5.8 (H10)	0.8	1 (H2), 2 (H4), 5 (H8, 8′), 9 (H10, 10)
H10, 10	3.74	5.9 (H9)	0.6	8 (H9)

* NOEs observed for the signals indicated when the proton at the left-hand side of the row is irradiated.

Table IV. ^{1}H NMR data (δ, *J*, T_1 and NOE) of IAA-L-Ile (**3**), in DMSO-d_6.

Proton	Chemical shift δ [ppm]	Coupling constant *J* [Hz]	Relax. time T_1 [s]	Nuclear Overhauser effects* NOE [%]
H1	10.82	–	0.9	9 (H2), 5 (H7)
H2	7.17	2.2 (H1)	1.9	6 (H1), 2 (H8, 8'), 1 (H13, 14)
H4	7.55	8.0 (H5)	1.7	8 (H5), 4 (H8, 8'), 1 (H13, 14)
H5	6.95	8.0 (H6), 8.0 (H4), 1.0 (H7)	1.4	10 (H4), 4 (H6)
H6	7.06	7.9 (H5), 7.9 (H7), 0.9 (H4)	1.5	9 (H7), 9 (H5)
H7	7.32	8.1 (H6), 0.7 (H1)	2.2	9 (H6), 3 (H1)
H8	3.55	14.8 (H8'), 0.5 (H2)	0.4	3 (H9), 2 (H4)**, 2 (H2)
H8'	3.62	14.8 (H8), 0.5 (H2)	0.4	
H9	8.04	8.5 (H10)	0.5	6 (H8, H8'), 5 (H13, 14), 1 (H2), 1 (H4), 2 (H10)
H10	4.19	8.5 (H9), 6.0 (H11)	1.1	5 (H13, 14), 5 (H11), 2 (H9)
H11	1.77	***	0.7	9 (H13, 14), 4 (H10), 3 (H9)
H12	1.16	***	0.4	10 (H11), 5 (H13, 14), 6 (H12')
H12'	1.39	***	0.4	2 (H13, 14), 7 (H12)
H13, 14	0.82	7.6 (H12)	0.6	14 (H12), 12 (H12), 16 (H11), 10 (H10), 2 (H4)

* NOEs observed for the signals indicated when the proton at the left-hand side of the row is irradiated.
** Simultaneous irradiation of both H-8.
*** Multiplets are not analyzed.

NOE techniques are unique in their ability to detect interactions between nuclei through space independent of the number of bonds between them. However, in reality, NOE conformational studies are complicated by numerous experimental difficulties [17]. Therefore, in the case of flexible molecules the prospects for a quantitative analysis are rather pessimistic.

The approach used in this study was confined to the consideration of NOEs as an information about which spins are close to each other. On this basis, it was possible to identify qualitatively conformations existing in the solution in considerable amounts, but it is extremely difficult to rule out the presence of small proportions of other conformers. It was advantageous that most of the compounds studied here showed restricted side-chain mobility.

Table V. ^{1}H NMR data (δ, *J*, T_1 and NOE) of IAA-L-Abu (**4**), in DMSO-d_6.

Proton	Chemical shift δ [ppm]	Coupling constant *J* [Hz]	Relax. time T_1 [s]	Nuclear Overhauser effects* NOE [%]
H1	10.84	–	0.8	4 (H7), 8 (H2), 1 (H12)
H2	7.19	–	1.9	6 (H1), 3 (H8, 8′), 1 (H9)
H4	7.57	7.9 (H5)	1.6	13 (H5), 2 (H8, 8′)
H5	6.91	7.8, 7.9 (H4, H6)	1.3	9 (H6), 11 (H4)
H6	7.06	8.0 (H5, H7)	1.4	14 (H5), 11 (H7)
H7	7.33	8.1 (H6), 0.7 (H1)	2.0	4 (H1), 12 (H6)
H8,	3.55	14.9 (H8′)	0.4	4 (H2)**, 4 (H4), 7 (H9)
H8′	3.60	14.9 (H8)	0.4	
H9	8.18	7.7 (H10)	0.5	2 (H4), 2 (H2), 3 (H10), 6 (H8, 8′), 3 (H12), 2 (H11), 1 (H11)
H10	4.14	***	1.3	4 (H11), 4 (H11′), 4 (H12), 2 (H9)
H11	1.63	***	0.4	5 (H11′), 11 (H12), 3 (H10), 2 (H9)
H11′	1.73	***	0.4	10 (H11), 9 (H12), 4 (H10), 1 (H9)
H12	0.86	7.4 (H11)	0.8	8 (H11), 8 (H11′), 2 (H1), 8 (H10)

* NOEs observed for the signals indicated when the proton at the left-hand side of the row is irradiated.
** Simultaneous irradiation of both H-8.
*** Multiplets are not analyzed.

*IAA-L-Alanine (IAA-L-Ala, **1**)*

There is a strong evidence for the trans-(E-)configuration of the side chain around the C9–N bond (torsional angle θ_3, Fig. 6) in this molecule (as in all others **2** to **7**) in solution: strong and mutual NOE enhancements (Table II) are observed between H8/H8′ and H9 (NH) (7–8%) but not between H8/H8′ and H10 as well as not between H8/H8′ and H11, *i.e.* the methyl protons of the alanine residue (see Fig. 6). Moreover, the NOE observed between H8/H8′ and H9 is consistent with a torsional angle of θ_2 = ca. 180° (*i.e.* opposite to the crystal structure, Fig. 2). On the other hand, the observed NOEs between H9 and H2 (ca. 1%), H9 and H4 (ca. 2%), H8/H8′ and H2 (2–5%), and H8/H8′ and H4 (5–6%) can only be accommodated in another conformation with θ_1 (C2–C3–C8–C9) ≈ ca. |90°| and θ_2 (C3–C8–C9–N) ≈ 0° (*i.e.* the same one which was observed in solid state [16], *cf.* Fig. 2). The observed ^3J(H9–H10) value of 7.3 Hz, the significant NOE between H9 and H10 (3–5%), as well as between the methyl protons and H9 (5%) are in agreement only with a θ_4 (C9–N–C10–C11) arrangement as depicted in Fig. 7:

Table VI. ^{1}H NMR data (δ, *J*, T_1 and NOE) of IAA-DL-Asp (**5**), in DMSO-d_6.

Proton	Chemical shift δ [ppm]	Coupling constant *J* [Hz]	Relax. time T_1 [s]	Nuclear Overhauser effects* NOE [%]
H1	10.83	–	0.8	5 (H7), 7 (H2)
H2	7.17	2.0 (H1)	1.8	6 (H1), 2 (H8, 8′)
H4	7.51	7.9 (H5)	1.7	13 (H5), 2 (H8, 8′)
H5	6.95	8.0 (H4, H6)	1.3	7 (H4), 5 (H6)
H6	7.03	8.1 (H5, H7)	1.4	4 (H5), 10 (H7)
H7	7.32	8.1 (H6), 0.7 (H1)	2.1	4 (H1), 9 (H6)
H8, 8′	3.54	–	0.6	3 (H2), 3 (H4), 3 (H9)
H9	8.26	7.9 (H10)	0.5	3 (H8, 8′), 3 (H10),
H10	4.54	7.1 (H11, H9)	1.2	2 (H9)
H11	2.59	16.6 (H11′)	0.3	21 (H11′), 3 (H9)
H11′	2.69	16.6 (H11), 5.6 (H10)	0.4	18 (H11)

* NOEs observed for the signals indicated when the proton at the left-hand side of the row is irradiated.

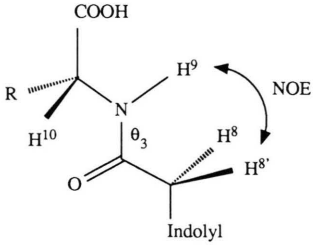

Fig. 6. Stereoprojection of partial structure of **1–7**.

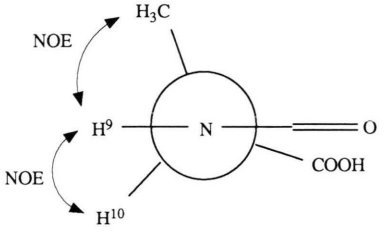

IAA-L-Ala (**1**), conformer with $\theta_2 \approx 180°$

Fig. 7. Newman projection of **1** (conformer with $\theta_2 = 180°$).

Here, the torsional angle between H9 and H10 is appr. 0° to −40° (for the conformer with $\theta_2 \approx 0°$) according to Bistrov's equation [18], a value of θ_4 which is close to the observed one in the solid-state structure of **1**.

The above results show that IAA-L-Ala (**1**) in DMSO-d_6 exists in a conformational equilibrium consisting mainly of two forms as a result of a rotation around θ_2 (≈ 0° and 180°, respectively). However, it should be noted that our results do not allow to decide whether θ_1 is ca. −90° (like in the solid state, Fig. 2) or +90° (rotation of the indolyl moiety by 180° with respect to the side chain). We assume that only these conformers are well-defined thermodynamically by virtue of steric and electrostatic (dipole-dipole) effects caused by the interactions between the mobile side chain and the indole moiety.

The observed NOEs in IAA-L-Ala in D_2O solution are qualitatively and quantitatively identical with those in DMSO-d_6 except that conversion of NH to ND cancels the respective NOE effects. This tends to support the conclusion that the conformations of IAA-L-Ala in the two solvents are identical.

Table VII. ^{1}H NMR data (δ, *J*, T_1 and NOE) of IAA-DL-Phe (**6**), in DMSO-d_6.

Proton	Chemical shift δ [ppm]	Coupling constant *J* [Hz]	Relax. time T_1 [s]	Nuclear Overhauser effects* NOE [%]
H1	10.79	–	0.8	8 (H2), 5 (H7)
H2	7.05	–	1.7	4 (H1)
H4	7.39	7.8 (H5)	1.7	18 (H5)
H5	6.90	7.9 (H5), 7.1 (H6)	1.3	9 (H6), 9 (H4)
H6	7.02	8.0 (H7), 0.9 (H4)	1.5	8 (H5), 8 (H7)
H7	7.30	8.1 (H6), 0.6 (H1)	2.1	3 (H1), 12 (H6)
H8, H8′	3.49	–	0.4	4 (H9), 2 (H4), 3 (H2)
H9	8.14	8.12 (H10)	0.5	3 (H8, H8′)
H10	4.43	**	1.0	1 (H11), 1 (H11′), 3 (H9), 4 (H12)
H11	2.86	9.3 (H10), 13.8 (H11′)	0.3	4 (H11′), 1 (H10)
H11′	3.03	4.8 (H10), 13.7 (H11)	0.3	11 (H11), 1 (H10)
H12 *(ortho)*	7.16	**	1.3	***
H13 *(meta)*	7.19	**	1.3	***
H14 *(para)*	7.16	**	1.6	***

* NOEs observed for the signals indicated when the proton at the left-hand side of the row is irradiated.
** Multiplets are not analyzed.
*** The resonances within the phenyl ring are too close to each other to display any NOE.

*IAA-Glycine (IAA-Gly, **2**)*

From the observed NOEs (Table III) it appears that the conformational behaviour of this molecule in DMSO-d_6 solution is the same as that of **1**.

*IAA-L-Ile (**3**)*

The NOEs and coupling constants monitored in DMSO-d_6 (Table IV) give evidence for a higher flexibility of the mobile side chain in comparison with **1**. The observed ^3J(H10,H11) = 6 Hz can be interpreted as an averaged value caused by a rotation around θ_5. There is also some evidence for different rotational properties of **3** with respect to the torsional angles θ_1 and θ_2. Thus, NOEs between H2 and H13/14 as well as H4 and H13/14 suggest that θ_1 is different from $|90°|$ and θ_2 different from 0° or 180°, namely $\theta_2 \approx -30°$ and +150°, respectively. Thus, in contrast to **1**, here we have an experimental proof that in solution the indolyl moiety may adopt two different orientations with respect to the asymmetric side chain. The weaker H9–H10 NOE enhancement in comparison with **1** and a ^3J(H9–H10) = 8.5 Hz suggest the torsional angle θ_4 between H9 and H10 to be in the range of 90°–180° instead of 0°–90° as observed in **1** (see Bistrov's equation [18]). So, this

Table VIII. ^{1}H NMR data (δ, *J*, T_1 and NOE) of IAA-δ-Ava (**7**), in DMSO-d_6.

Proton	Chemical shift δ [ppm]	Coupling constant *J* [Hz]	Relax. time T_1 [s]	Nuclear Overhauser effects* NOE [%]
H1	10.83	–	0.9	4 (H11, 11′), 4 (H10, 10′), 8 (H5), 8 (H2), 8 (H7)
H2	7.16	2.3 (H1)	2.0	3 (H11, 11′, 12, 12′), 2 (H8, 8′), 7 (H1), 1 (H10, 10′)
H4	7.53	7.8 (H5)	1.7	14 (H5), 2 (H8, 8′)
H5	6.95	7.93 (H4, H6), 1.0 (H7)	1.4	11 (H6), 12 (H4)
H6	7.05	8.0 (H5, H7), 1.1 (H4)	1.5	8 (H5), 12 (H7)
H7	7.32	8.1 (H6), 0.8 (H1)	2.2	12 (H6), 4 (H1)
H8, 8′	3.47	–	0.5	3 (H13), 4 (H2), 4 (H4), 7 (H9), 3 (H10), 5 (H11)
H9	7.87	5.5 (H10)	0.6	7 (H10), 4 (H11), 5 (H8, 8′), 2 (H13, 13′)
H10, 10′	3.02	5.5 (H9)	0.5	4 (H13), 8 (H12), 7 (H11), 5 (H9)
H11, 11′	1.40	**	0.5	9 (H13), 16 (H10), 4 (H9)
H12, 12′	1.47	**	0.5	17 (H13), 13 (H10), 1 (H8, 8′), 2 (H2) 4 (H9)
H13, 13′	2.18	7.2 (H12)	0.7	8 (H11, 11′, 12, 12′)

* NOEs observed for the signals indicated when the proton at the left-hand side of the row is irradiated.
** Multiplets are not analyzed.

torsion angle can be estimated to be ca. −150° (Fig. 8a), the same as in the crystal structure of **3** [16].

*IAA-L-α-Aminobutyric Acid (IAA-L-Abu, **4**)*

The conformational features of the side chain in **4** are similar to those in **3** (Fig. 8a). The NOEs (Table V) between H9 and H2 (1−2%) as well as H9 and H4 (1−2%) suggest some rotational freedom around the torsional angles θ_1, θ_2, θ_4, and θ_5. The H9−H10 NOE effect (2−3%) and the value of ^3J(H9−H10) = 7.7 Hz render the torsional angle θ_4 ca. −150° like in the case of **3** (Fig. 8a).

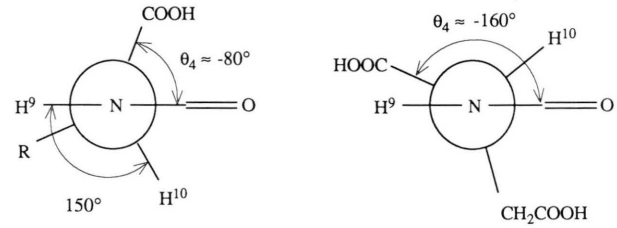

a — IAA-L-Ile (**3**), IAA-L-Abu (**4**)

b — IAA-L-Asp (**5**)

Fig. 8. Newman projections, (a) **1** ($\theta_2 = 0°$), **3** and **4**, (b) **5**.

*IAA-DL-Aspartic Acid (IAA-DL-Asp, **5**)*

Similar to the situation in the case **1**, a conformer with $\theta_1 \approx 90°$ is present because significant NOE of 2–3% are found for the pairs H8–H2, H8–H4. Overhauser effect are present between H9 and H8 (3%) proving the existence of a trans-arrangement for θ_2, a finding again in contrast to that in the solid state (Fig. 8). The presence of the respective cis-conformer cannot be ascertained by our experiments.

The molecule shows some conformational restriction about the torsional angles θ_4 and θ_5 with predominance of the conformation observed by the X-ray analysis (Fig. 8b). There are two vicinal coupling interactions between the H10 and the two H11 protons (6.8 and 5.6 Hz) and the value of ^3J(H9–H10) is 7.8 Hz.

*IAA-DL-Phenylalanine (IAA-DL-Phe, **6**)*

As for 5, NOEs were detected between H8/H8′ and H2 (3%), H8/H8′ and H4 (2%) as well as H8/H8′ and H9 (3–4%) but not between H9 and H2 or H9 and H4 suggesting that θ_1 is predominantly *ca.* 90° and θ_2 ca. 180°. In addition, weak NOEs are observed between H10 and the two anisochronous H11 protons. The vicinal coupling constant ^3J(H9–H10) is 8.2 Hz and two different ^3J were measured between H10 and the two H11 protons (9.8 and 4.8 Hz). Moreover, no NOEs were observed between the protons of the two benzene rings (from the side chain and the indole ring) but a shielding effect is present for H4 and H5. All these data can be related to a conformationally restricted structure of **6** in solution, without any hydrogen-bonding between the CO and COOH groups as shown in Fig. 9.

*IAA-δ-Aminovaleric Acid (IAA-δ-Ava, **7**)*

The NOEs H8/H8′ and H2 (3%), H8/H8′ and H4 (3%) as well as H8/H8′ and H9 (5–7%) suggest again a preferred conformational behaviour about θ_1, θ_2, and θ_3 similar to that of **1**, **5**, and **6**. This time, those findings are consistent with the conformation obtained in solid state (Fig. 5).

However, there are significant NOE signal enhancements for the pairs H9 and the two H10 (5–7%) as well as H9 and the two H11 (4%). The first indicates a *cis*-arrangement around θ_4, the second a *trans*-arrangement for the same fragment. Additional NOEs between the atoms H9, H11, H12 and H13 confirm the flexibility of this part of the side chain.

Structure-activity relationships

IAA amino acid conjugates promote growth in plant stem sections, and they influence callus prolif-

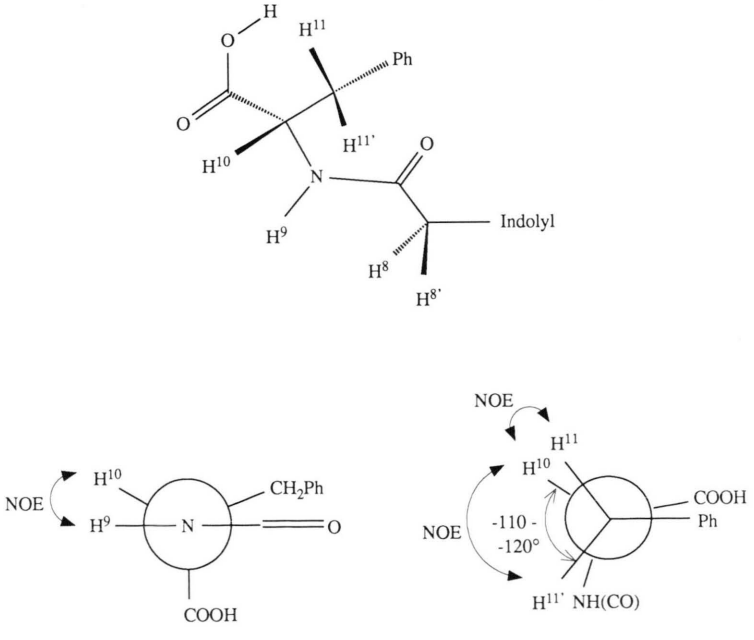

Fig. 9. Newman and stereoprojections of **6**.

eration and organogenesis in plant tissue culture [5, 6, 19]. The different steady state concentrations of free auxin formed by enzymatic hydrolysis of the individual conjugates appear to be the main factor determining their physiological activities, which depend on both their structures and the plant system [5, 20]. A further step towards the growth response would be binding of the IAA liberated to one or more of the auxin receptor proteins, three types of which have so far been described [2]. Competition of free and conjugated IAA at the receptor sites is a possibility rarely considered, although it would readily explain the specific interaction of free and bound auxin in some plant systems [6, 21].

Because of this complex mechanism of action, it is difficult to correlate the structures and physiological activities of IAA amino acid conjugates. A further obstacle is the fact that the seven compounds studied here have not been assayed in the same plant system. In *Solanum nigrum* callus [6] IAA-Ala was most active, while the concentrations necessary to achieve a comparable physiological response (half-optimal callus weight) were about 10-fold for IAA-L-Abu, 30-fold for IAA-Gly and IAA-δ-Ava, and 100-fold for IAA-L-Ile. In soybean cotyledon callus [19], 200 times the amount of IAA-Asp was required to match the effect of IAA-Ala, while the two conjugates were of equal activity in *Avena* coleoptyles [19]. IAA-Phe was very inactive (numerical values not provided) in both systems [19].

This work is only a first attempt to obtain some insight into structure-activity relationships for IAA conjugates. It appears that, in solution, the hydrophobic tails of the long-chain aliphatic amino acids tend to cluster around the indole ring while the −CONH− and COOH groups tend to converge into a hydrophilic pole, thus rendering the molecules exceedingly amphipatic. Such conjugates would then tend to concentrate in lipoid-aqueous phase boundaries rather than in aqueous solution, such as in the cell vacuole, which may compartementalize them away from hydrolytic enzymes. This could explain their poor physiological activity. Also, at the active site of an enzyme which can optimally accommodate the relatively water-soluble IAA-Ala, an additional energy input may be required for the higher amino acids to achieve the orientation at the protein surface required for cleavage of the amide bond. The benzene ring in IAA-Phe, although not too close to the indole moiety, is still on the same side of the molecule in solution. It is apparently locked in that position, and it is more rigid than an aliphatic side chain. So this compound may well be the most amphipatic, as it is the least active of the conjugates studied here. IAA-Asp is normally formed by plants to regulate endogenous auxin levels. So its hydrolysis should be the task of special housekeeping enzymes, which may well be different from those cleaving the other amino acid conjugates considered in this work.

Another way to look at the data obtained would be to view IAA amino acid conjugates as models for IAA bound to a receptor protein. There are indeed good reasons to assume that the carboxyl group is a primary binding site (most active auxins are acids), although no amide bond is formed at the receptor (binding is reversible). The hydrophobic tails of the binding and neighbouring amino acids would then tend to cluster around the indole ring in specific patterns, as they do in IAA conjugates with i-leucine (Ile), α-aminobutyric acid (Abu) and δ-aminovaleric acid (δ-Ava). This could, at least in theory, be the way how a receptor site recognizes IAA, while many structurally related compounds could also be adopted with relatively low energy input for deformation of the flexible aliphatic tails of the respective amino acids.

Acknowledgements

M.F.S. thanks the Heinrich-Hertz foundation for granting a study-leave to Bochum university. B.K.-P. gratefully acknowledges support from Internationales Büro, Kernforschungsanlage Jülich (bilateral scientific and technical cooperation between the F.R.G. and Yugoslavia). This work was supported by the Fonds der Chemischen Industrie.

[1] F. Kögl, A. J. Haagen-Smit, and H. Erxleben, Hoppe-Seyler's Z. Physiol. Chem. **228,** 90 (1934).
[2] Plant Hormones and Their Role in Plant Growth and Development (P. J. Davies, ed.), Martinus Nijhoff, Dordrecht 1987.
[3] N. G. Cholodny, Planta **23,** 289 (1935).
[4] J. D. Cohen and R. S. Bandurski, Ann. Rev. Plant Physiol. **33,** 403 (1982), and references therein.
[5] R. P. Hangarter, M. D. Peterson, and N. E. Good, Plant Physiol. **65,** 761 (1980); R. P. Hangarter and N. E. Good, Plant Physiol. **68,** 142 (1981).
[6] V. Magnus, R. P. Hangarter, and N. E. Good, to be published.
[7] S. P. Singh, S. S. Parmer, V. J. Stenberg, and S. A. Farnum, J. Heterocycl. Chem. **15,** 13 (1978); J. Vebrel, B. Laude, A. Seguin, and J. Dubouchet, Spectrochim. Acta **39A,** 887 (1983).
[8] R. G. Parker and J. D. Roberts, J. Org. Chem. **35,** 996 (1970).
[9] R. Richarz and K. Wüthrich, Biopolymers **17,** 2133 (1978).
[10] A. Bundi and K. Wüthrich, Biopolymers **18,** 285 (1979).
[11] A. Evidente, G. Surico, N. S. Iacobellis, and G. Randazzo, Phytochemistry **25,** 125 (1986).
[12] E. A. Schneider and F. Wightmann, Phytohormones and Related Compounds – A Comprehensive Treatise, **Vol. 1,** Elsevier, Amsterdam 1978.
[13] T. Wieland and G. Hörlein, Liebigs Ann. Chem. **591,** 192 (1955).
[14] N. E. Good, Can. J. Chem. **34,** 1356 (1956).
[15] S. Fuchs, J. Haimovich, and Y. Fuchs, Eur. J. Biochem. **18,** 384 (1971).
[16] B. Kojic-Prodic, B. Nigovic, Z. Ruzic-Toros, and V. Magnus, Z. Kristallogr. **185,** 493 (1988).
[17] J. K. M. Sanders and B. K. Hunter, Modern NMR Spectroscopy, p. 163–205, Oxford University Press 1987.
[18] V. F. Bystrov, V. T. Ivanov, S. L. Portnova, T. A. Balashova, and Yu. A. Ovchinnikov, Tetrahedron **29,** 873 (1973).
[19] C.-S. Feung, R. H. Hamilton, and R. O. Mumma, Plant Physiol. **59,** 91 (1977).
[20] K. Bialek, W. J. Meudt, and J. D. Cohen, Plant Physiol. **73,** 130 (1983).
[21] T. J. Wodzicki, R. P. Pharis, and A. B. Wodzicki, Plant Physiol. **84,** 1139 (1987).